Tropical Atlantic Moisture Flux, Convection over Northeastern Brazil, and Pertinence of the PIRATA Network

Bruno Durand, Jacques Servain, Henri Laurent, Luiz A. T. Machado

Tropical Atlantic Moisture Flux, Convection over Northeastern Brazil, and Pertinence of the PIRATA Network*

BRUNO DURAND

Fundação Cearense de Meteorologia e Recursos Hídricos (FUNCEME), Fortaleza, Ceará, Brazil

JACQUES SERVAIN

Institut de Recherche pour le Développement (IRD), Paris, France, and Fundação Cearense de Meteorologia e Recursos Hídricos (FUNCEME), Fortaleza, Ceará, Brazil

HENRI LAURENT

Institut de Recherche pour le Développement (IRD), Paris, France, and Centro Técnico Aeroespacial/Instituto de Aeronautica e Espaço/Divisão de Ciências Atmosféricas (CTA/IAE/ACA), São José dos Campos, Brazil

LUIZ A. T. MACHADO

Centro Técnico Aeroespacial/Instituto de Aeronautica e Espaço/Divisão de Ciências Atmosféricas (CTA/IAE/ACA), São José dos Campos, Brazil

(Manuscript received 9 December 2003, in final form 13 October 2004)

ABSTRACT

This study aims to examine the relationship between the tropical Atlantic latent heat flux and convective cloud coverage over northeast Brazil (NEB) during the four months of the main rainy season (February–May). The correlation with anomalies of these data is investigated, both without lag and with a 1-month lag (the heat flux in advance). In both cases, a significant positive correlation appears in the northwestern tropical Atlantic, and a significant negative correlation is obtained for a limited area off eastern NEB. These two correlation patterns are linked to anomalies in the trade wind intensity and in the meridional position of the intertropical convergence zone (ITCZ), which relate to the latent heat flux anomalies and NEB convective coverage anomalies, respectively. The positive correlation pattern is spread over a large part of the northern tropical Atlantic, whereas the negative correlation pattern is confined off NEB. This indicates the existence of different regional mechanisms in the tropical Atlantic basin. The impact of the Atlantic heat fluxes on NEB convection is somewhat different from the classical meridional dipole related to the SST variability. The analysis of the horizontal moisture flux shows that during flood years an additional meridional inflow balances the eastward loss, and the upward velocity reinforced over NEB contributes to intensify NEB convection. The positive correlation pattern indicates that the location of the northern branch of the Pilot Research moored Array in the Tropical Atlantic (PIRATA) moorings is pertinent to monitor the ocean–atmosphere interface parameters. The negative correlation pattern off NEB provides new support for the possible extension of the PIRATA array toward the Brazilian coast. Complementary results at 1-month lag and the real-time availability of the PIRATA data confirm the potential of NEB forecasting.

1. Introduction

The northern northeast Brazil (NNEB) precipitation regime, with its main rainy season from February to May (Strang 1972), is the predominant rainfall regime in the northeast Brazil (NEB) semiarid region (Kousky 1979). February–March–April–May (FMAM) is the period of the year when the intertropical convergence zone (ITCZ) attains its southernmost position, reaching

* Conselho Nacional de Desenvolvimento Científico e Tecnológico–Institut de Recherche pour le Développement Contribution Numbers 910072/00-0 and 690089/01-5.

Corresponding author address: Dr. Bruno Durand, FUNCEME, Av. Rui barbosa, 1246-Aldeota, Fortaleza, Ceará 60115-221, Brazil. E-mail: bruno@funceme.br

the NEB (Hastenrath and Heller 1977). The high interannual rainfall variability shows normal years interspersed with drought and flood years, and has consequent economic and social impacts. Several studies have related this interannual variability to ocean parameters such as sea surface temperature (SST). Correlation studies (Hastenrath and Heller 1977; Moura and Shukla 1981) between SST anomalies and rainfall anomalies over NEB highlighted a dipolelike pattern straddling the ITCZ. Negative (positive) SST anomalies in the southern tropical Atlantic and positive (negative) anomalies in the northern tropical Atlantic are associated with drought (humid) years. Chung (1982) linked SST, wind, and precipitation in NEB, showing that stronger than normal trade winds in the South Atlantic take place in the months preceding the FMAM rainy season during drought years. Hastenrath and Heller (1977) associated anomalously dry years with a weakening of the equatorward part of the North Atlantic subtropical high, an equatorward expansion of the South Atlantic subtropical high, and an anomalous northward position of the ITCZ. They obtained opposite patterns for abundant rainy seasons.

Droughts and floods in the NEB are also related with the phases of El Niño–Southern Oscillation (ENSO). During a warm ENSO episode (El Niño event), the Walker cell migrates eastward causing anomalous subsiding motions over the Amazon, NEB, and tropical Atlantic, thus reducing precipitation. On the other hand, during a cold ENSO episode (La Niña) vertical motion is increased over those regions, with more rainfall. Significant links between ENSO events and precipitation in the NEB region are found in numerical modeling experiments and observation (Harzallah et al. 1996; Roucou et al. 1996). Those authors have also shown that anomalies in the SST field in the tropical Atlantic change the Hadley cell in such a way as to cause anomalous subsidence in dryer than normal years and accelerated vertical motion in years with an excess of rainfall over the NEB.

Fluxes at the ocean–atmosphere interface—latent and sensitive heat fluxes, and momentum flux—are essential parameters for ocean–atmosphere interaction studies. In a sensitivity study, Wang et al. (1996) showed that the latent heat flux is the most significant of the three fluxes mentioned above, when considering the structure and the internal dynamics of intense convective systems. Studies performed in the context of the Tropical Ocean Global Atmosphere Coupled Ocean–Atmosphere Response Experiment (TOGA COARE) in the Pacific have shown the influence of heat fluxes on convection, which is directly linked to precipitation. These fluxes are significant in the atmosphere carrying humidity and heat, which are necessary for the development of convection and precipitation (Rotunno and Emanuel 1987; Tao et al. 1991). On the other hand, atmospheric conditions such as wind, cloud coverage, and precipitation affect ocean surface parameters by altering the fluxes (Webster and Lukas 1992).

This preliminary work aims at studying the relationship between observations of the tropical Atlantic latent heat flux and the convective systems over NEB. The convective cloud coverage data used here are available on a 2.5° horizontal grid. This limited us to a better definition of the NEB. We defined this region between 10°S and the northern coast, and between 45°W and the eastern coast (see maps in Fig. 1). We try to answer the following questions: What is the impact of the tropical Atlantic heat fluxes on NEB convection? What is the relative importance of the strong latent heat fluxes on both sides of the ITCZ? Could the link between latent heat flux and NEB convection lead to potential forecast applications?

To measure variables of the ocean–atmosphere interaction in the tropical Atlantic, an observational network has been set up, the Pilot Research moored Array in the Tropical Atlantic (PIRATA; Servain et al. 1998). The locations of the moorings (see Fig. 1) have been chosen to monitor the two main modes of the tropical Atlantic variability—the meridional mode and the equatorial mode (Servain et al. 2000). Here we will also investigate whether the locations of the moorings are adequate for study of the relationships between heat fluxes and NEB convection.

The data used in this study, the climatology during the FMAM season, and the methods of calculations are presented in section 2. In section 3, we present correlation of the tropical Atlantic latent heat flux anomalies with the NEB convective cloud coverage anomalies during the rainy season without lag and with 1-month lag (the heat flux in advance). Section 4 is a discussion of these results, before the conclusions in section 5.

2. Data and methods

We decided to base this preliminary study on observation data. This criterion restricted the data choice and the period of study. After a comparative study between three latent heat flux datasets (Durand et al. 2002), we chose the da Silva latent heat flux dataset (da Silva et al. 1994), based on in situ observations (merchant ship data). These data are available monthly from 1945 to 1995 on a 1° global grid. Here, positive heat fluxes mean a heat transfer from the ocean toward the atmosphere. Thus, in the correlation study (section 3), when we mention positive (negative) flux anomalies

that means a positive (negative) energy transfer into the atmosphere.

Machado et al. (2004) justified the use of convective cloud cover to define the rainy season. They obtained a good relationship between precipitation and convective cloud cover on a monthly scale. The use of cloud coverage data gives a simple and objective approach, and the spatial cover avoids extrapolations that may be spurious in case of few rain gauge measurements. The convective cloud coverage data are derived from satellite observations and processed by the International Satellite Cloud Climatology Project (ISSCP; Schiffer and Rossow 1985). To describe only the clouds with convective activity, we used the cloud coverage with cloud-top pressure smaller than 310 hPa. The data are available on a 2.5° grid, every 3 h, from 1983 to 1994. The heat flux data temporal resolution is monthly, so we calculated monthly means of the convective cloud coverage. Taking into account the temporal limitations of both datasets, we have at our disposal a 10-yr data period, from 1984 to 1993. We defined the NEB region as the area located between 10°–2.5°S and 45°–35°W (i.e., 11 grid points). We averaged the monthly convective cloud coverage of these 11 grid points, and defined a NEB convective cloud coverage index as the normalized anomalies (anomalies divided by the standard deviation) of this monthly series.

For discussion and interpretation of the results we used also data from the monthly National Centers for Environmental Prediction–National Center for Environmental Prediction (NCEP–NCAR) reanalysis (Kalnay et al. 1996): the wind field, the vertical velocity, and the specific humidity (between 1000 and 300 hPa). The low-level wind data is used to define the ITCZ position as the quasi-zonal line where the meridional component is zero. We calculated the horizontal moisture flux as the horizontal wind multiplied by the specific humidity.

Figure 1 shows the FMAM climatology of (Fig. 1a) latent heat flux and (Fig. 1b) convective cloud coverage. The FMAM climatology of the NCEP–NCAR 925-hPa-level wind field and the FMAM climatological position of the ITCZ, are also represented.

The latent heat flux FMAM climatology (Fig. 1a) shows large values on both sides of the ITCZ. Over the ocean, the ITCZ (i.e., the region of maximum convection) is also the region of low-level wind confluence. On both sides of the ITCZ, trade winds are strong and the relatively weak cloud coverage allows a large amount of solar radiation to reach the surface. However, given the total cloud coverage climatology (not represented here), the regions of maximum latent heat flux do not coincide exactly with the regions of minimum cloud coverage. This suggests that wind is the most important parameter that modulates the flux intensity.

The FMAM climatology of convective cloud coverage (Fig. 1b) shows a large convective cloud coverage maximum (mean values between 20% and 30% of the total surface) spreading over the Amazon and the NNEB. Over the ocean, convective cloud coverage values are smaller, but the ITCZ appears clearly as the region of maximum convection over the tropical Atlantic. Values up to 20% are observed between 7°S and 5°N on the western part of the Atlantic and between the equator and 5°N on the eastern part.

3. Results

To analyze the relationships between the latent heat flux and the convective cloud coverage, we calculated the correlation between their monthly anomalies. The two datasets are characterized by strong seasonal cycles, which contribute to a large portion of their correlation, hiding the signal of the correlation based on the nonseasonal variability. Calculating the correlation with normalized anomalies (monthly value minus monthly climatology divided by the standard deviation of the month) eliminates the contribution of the seasonal cycle. Two kinds of correlation are calculated: one with a time series without lag and the other with 1-month lag. Hereafter, when speaking of 1-month lag correlation, it means that the heat flux is in advance with respect to the convective parameter. For the in-phase correlation, both the heat flux and convective cloud time series are made up of monthly values from FMAM of each year from 1984 to 1993 (i.e., 40 values). For the 1-month lag correlation, the convective cloud time series is again composed of monthly values from FMAM, while the heat flux time series is now made up of monthly values from January to April. The significance of the correlation is estimated with the Student's t test. With series of 40 values, correlations larger than 0.31, in absolute value, are 95% significant.

Figure 2 shows maps of correlation, (Fig. 2a) in phase and (Fig. 2b) with a 1-month lag, between the latent heat flux anomalies of the whole tropical Atlantic Ocean and the convective cloud coverage anomalies over NEB during the rainy season. In these maps only the 95% significant correlation values are shaded. We chose two 5° × 5° squares in the regions of maximum in-phase and 1-month lag correlation (12.5°–17.5°N, 40°–35°W and 2.5°–7.5°N, 40°–35°W, hereafter PIRATA1 and PIRATA2, respectively). In the same way, we calculated the NEB convective cloud index by averaging the monthly latent heat flux series in these two regions and calculating their normalized anomalies. Note that these two specific areas are located along the

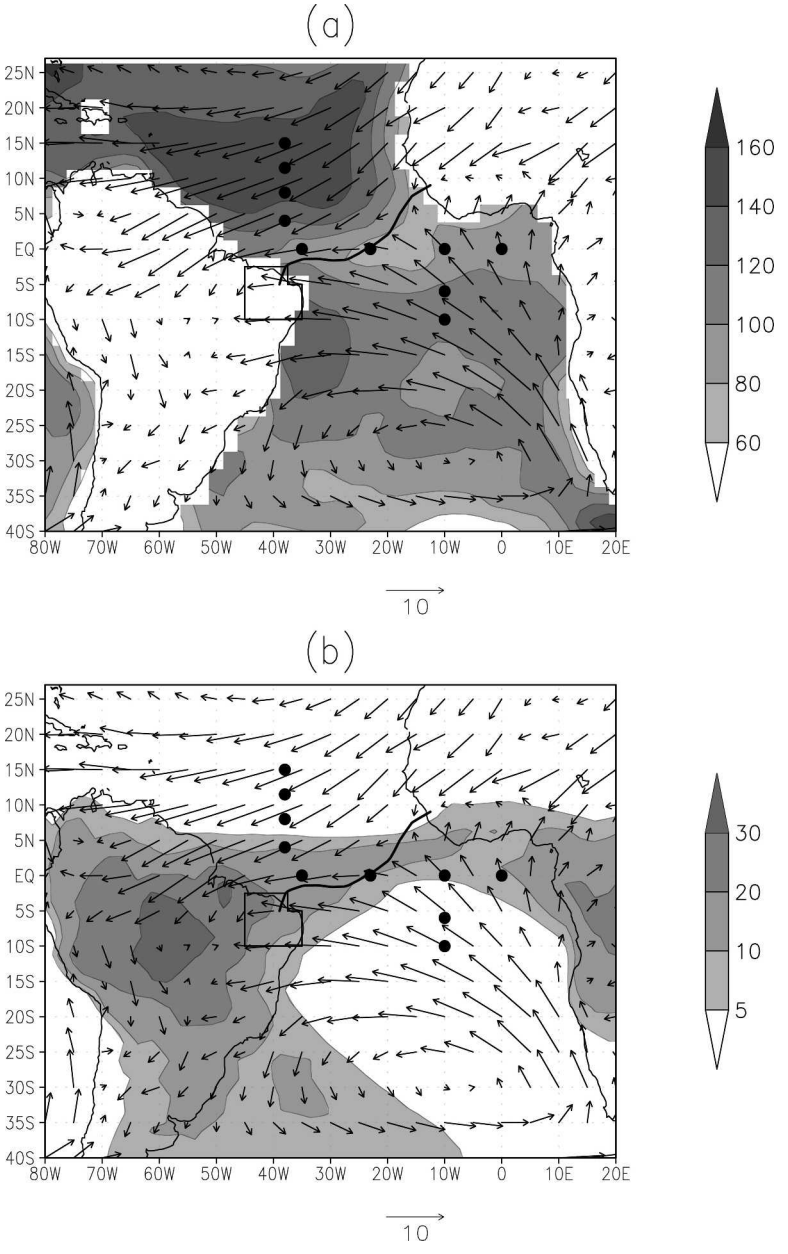

FIG. 1. The FMAM climatology of (a) the da Silva latent heat flux (W m^{-2}) and (b) the convective cloud coverage (%). The FMAM climatology of the wind field at 925 hPa is also plotted. The black polygon delimits NEB, and the full black circles indicate the position of the PIRATA buoys. The thick line is the climatological position of the ITCZ during FMAM months.

northern branch of the PIRATA network. Figures 2c,d show the FMAM NEB convective cloud coverage anomaly index (solid line); furthermore (Fig. 2c) shows the FMAM PIRATA1 heat flux index (dashed line), and (Fig. 2d) shows the JFMA PIRATA2 heat flux index shifted forward by 1 month (dashed line).

These maps help to determine which regions of the tropical Atlantic are linked (with regard to the surface latent heat flux) to the NEB convective coverage variability. The correlation in phase (Fig. 2a) shows a strong signal of positive correlation in the northwestern tropical Atlantic with a maximum (greater than 0.6) in the vicinity of 15°N, 38°W where a PIRATA mooring is located. The correlation decreases when approaching the northern coast of South America. Off the NEB, in the region between 2°and 12°S, and between the Bra-

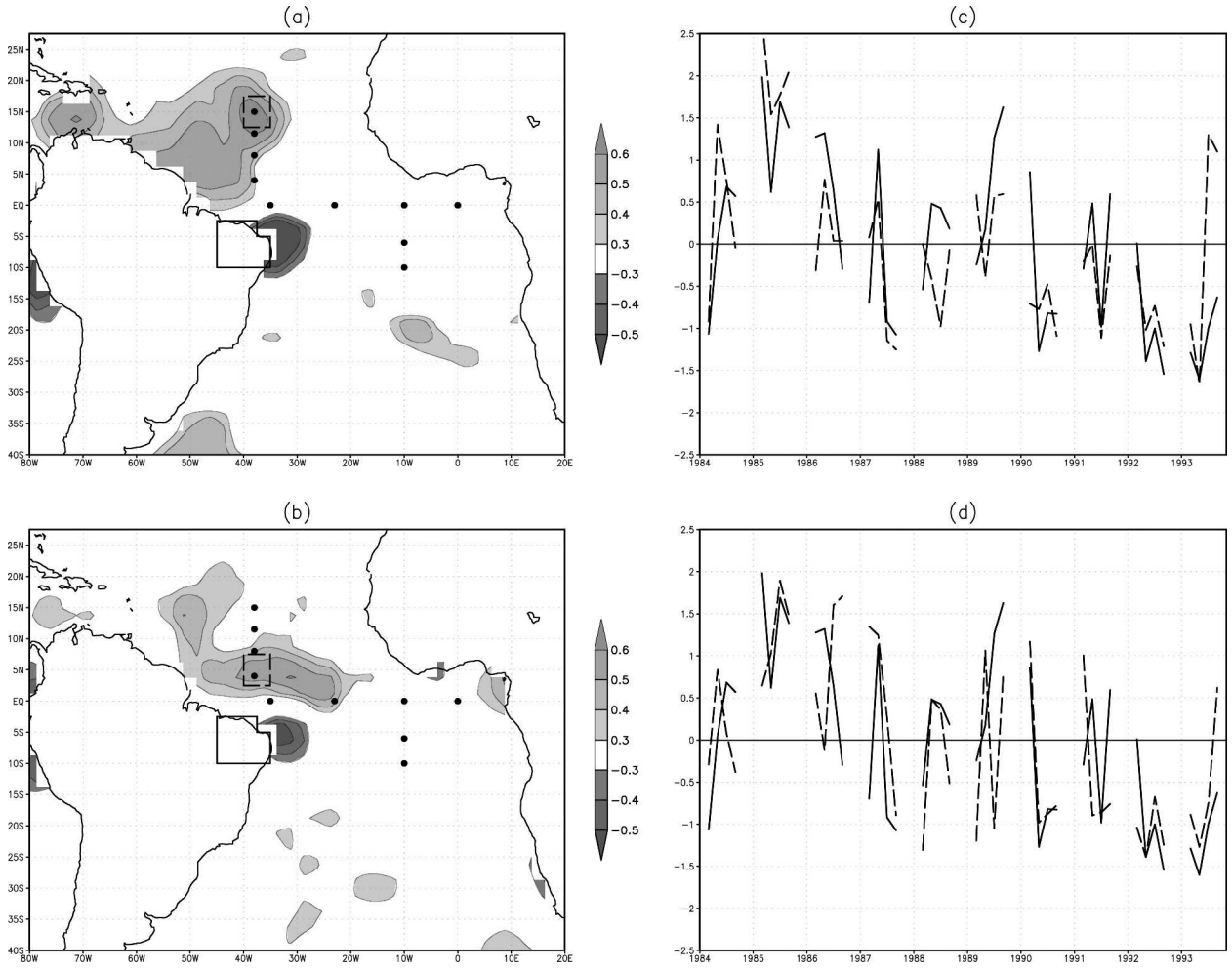

FIG. 2. (a) Correlation of the monthly mean anomalous values of the NEB convective cloud coverage with the tropical Atlantic latent heat flux anomalous values for FMAM during the 1984–93 period (the anomalies are normalized by the std dev); (b) the same as (a) with the NEB convective cloud cover in the months FMAM and the tropical Atlantic heat flux in the months JFMA (1-month lag). Only the 95% significant correlation values are shaded. The black polygon delimits NEB, and the full black circles indicate the position of the PIRATA buoys. FMAM NEB convective cloud index (solid line) is superimposed to (c) FMAM latent heat flux index (dashed line) of the area between 12.5°–17.5°N and 40°–35°W and to the (d) JFMA latent heat flux index (dashed line) of the area between 2.5°–7.5°N and 40°–35°W and shifted forward by 1 month. The dashed square in (a), (b) indicates the area in which we calculated the latent heat flux index in (c), (d).

zilian coast and 30°W, there is a large negative correlation area up to −0.5 near the coast. Those positive and negative correlation areas outline a meridional dipolelike pattern.

A large positive correlation area is also observed in the northwestern tropical Atlantic for a 1-month lag (Fig. 2b) although with a few differences. This 1-month lag correlation is weaker than the in-phase correlation, except in the region between 40° and 30°W and along 5°N, where the maximum 1-month lag correlation is located, reaching values between 0.5 and 0.6. The 1-month lag correlation maximum is located at 5°N near the PIRATA mooring at 4°N, 38°W, which is contrary to what is observed for the in-phase correlation where the maximum occurs in the vicinity of 15°N. A significant negative correlation pattern is located off NEB, in the same region as the in-phase pattern.

Figures 2c,d show a significant agreement between the FMAM NEB convective cloud index and the FMAM PIRATA1 and JFMA PIRATA2 latent heat flux indexes. During a few years, 1987, 1991, 1992 (in Fig. 2c) and 1990, 1992, 1993 (in Fig. 2d), the two indexes are indeed similar, which shows that the latent heat flux variability in the region of the PIRATA northern branch is highly pertinent to the study of the NEB convection variability.

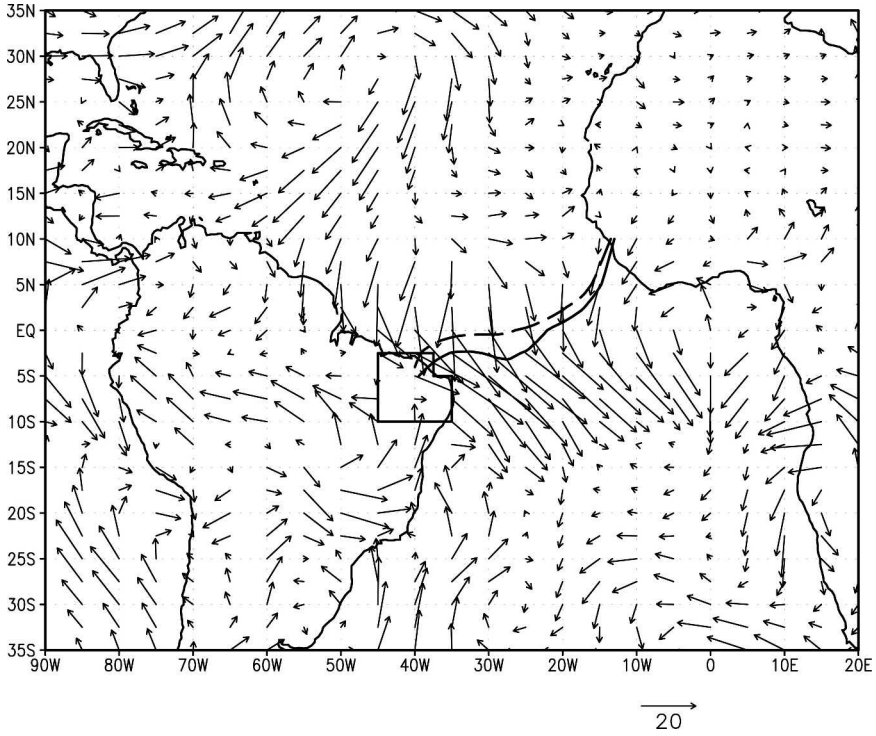

FIG. 3. Bias of the FMAM 1000-hPa horizontal moisture flux (10^{-3} g kg^{-1} m s^{-1}) between flood and drought years. The solid (dashed) line indicates the average ITCZ position for FMAM of the five flood (drought) years. The black polygon delimits the region defining NEB.

4. Discussion

We averaged the convective cloud coverage both in space (over NEB), and in time (during the rainy season of FMAM for each year). We thus obtained a 10-value series (1 value per year during the period 1984–93), characterizing the intensity of the FMAM NEB convection. During this period, 5 yr are characterized by a more intense FMAM convection over NEB (1984, 1985, 1986, 1988, and 1989), hereafter named "flood years," and the other five (1987, 1990, 1991, 1992, 1993), hereafter named "drought years," present weaker values. During the FMAM main rainy season, precipitation is largely due to the convective activity of the ITCZ, reaching NEB in this season. See Fig. 3 for the average position of the ITCZ during the five flood (drought) years represented by a solid (dashed) line.

The composite anomalies of the NCEP–NCAR surface wind field (not shown here) for rainy (drought) years show stronger (weaker) trade winds in the Northern Hemisphere, and weaker (stronger) trade winds in the Southern Hemisphere. This anomaly in the wind field is associated with an abnormal southward (northward) displacement of the ITCZ. This is coherent with the results obtained by Hastenrath and Heller (1977), showing that during abnormally rainy (drought) years over NEB, the ITCZ is southward (northward) of its average position. During the years of positive (negative) convective coverage anomaly, stronger (weaker) trade winds in the Northern Hemisphere imply a positive (negative) latent heat flux anomaly in this region, and weaker (stronger) southern trade winds will induce a negative (positive) latent heat flux anomaly off the NEB eastern coast. This simultaneously explains the positive correlation pattern in the northwestern tropical Atlantic and the negative correlation pattern off NEB (Fig. 2).

To better understand the mechanisms that feed convection over NEB, and how convection increases during flood years, we calculated the horizontal moisture flux from the NCEP–NCAR data (as the horizontal wind multiplicated by the specific humidity). We calculated the difference of the FMAM 1000-hPa horizontal moisture flux between flood and drought years (Fig. 3).

Below, an analysis is made based on flood years, and we comment on phenomena associated with them. For drought years, we obtain opposite patterns. The difference of the horizontal moisture flux between flood and drought years is coherent with the surface wind anomalies (not shown) described previously. Figure 3 clearly

shows the intensification of the North Atlantic subtropical high, the southward displacement of the ITCZ, the intensification of the northern trade winds, and the decreasing of southern trade winds, which are all characteristic of flood years.

The FMAM horizontal moisture flux climatology (not shown here) shows that the westward moisture flux from the ocean is the main contribution to NEB. But Fig. 3 clearly shows that flood years are characterized by an eastward anomaly. In these years, the additional moisture necessary to feed NEB convection seems to come from the meridional contribution: both the southward flux near the NEB northern coast between 10°N and 0° and the northward flux south of NEB increase the meridional moisture contribution during flood years. Thus, the total NEB moisture amount is larger and can feed convection.

To confirm this explanation, we extracted (from the NCEP–NCAR data) vertical profiles between 1000 and 300 hPa of the zonal moisture flux (averaged between 10°S and 0°) and of the meridional moisture flux (averaged between 45° and 35°W), and plotted the difference between FMAM of flood and drought years (Figs. 4a,b, respectively) of these two variables. These figures also represent the difference in vertical velocity between flood and drought years (with the same spatial averages). Note that negative values of the vertical velocity indicate an upward movement. It is important to underline the fact that zonal flux is positive when it is eastward, and meridional flux is positive when it is northward.

In the region between 43° and 2°W, the difference of the zonal moisture flux between flood and drought years is positive (Fig. 4a), showing a reduced zonal moisture contribution during flood years, as observed before. The difference is more intense at low levels (from the 1000–850-hPa level). A negative zonal flux difference, west of 45°W indicates an enhanced westward zonal flux to the west of NEB. Flood years are also characterized with a reinforced ascending motion between 40° and 30°W, with maximum values above 35°W, which is the eastern part of NEB.

During flood years, the meridional moisture flux (Fig. 4b) is characterized by intensification of the southward flux between 10°N and 5°S and of the northward flux, south of 10°S. These anomalies are larger at low levels (from the surface to 850 hPa for the southward contribution, and from the surface to 700 hPa for the northward one). This phenomenon is associated with enhanced ascending motion in the region centered on 0°–5°S, corresponding to the southward displacement of the ITCZ in flood years.

These profiles show that although the westward moisture contribution in NEB is smaller during flood years, this loss is balanced by an additional meridional moisture contribution from both north and south. This larger total NEB moisture amount, associated with increased ascending motion, allows a more intense convective activity and more precipitation.

The positive correlation pattern located in the northwestern tropical Atlantic (Fig. 2) is not a causal relationship, but results from the fact that heat flux anomalies in this region and the NEB convection anomalies are linked to the same atmospheric modification, intensification of the northern trade winds, and southward shift of the ITCZ during flood years.

The negative correlation pattern obtained in the vicinity of NEB's eastern coast (Fig. 2) is unexpected at first sight: less latent heat in NEB vicinity can appear to be in contradiction with more convection and rain in NEB. In fact, flood years are characterized by a modification of the atmospheric circulation, reinforcing northern trade winds, and decreasing southern trade winds. Thus the latent heat flux off NEB and the westward moisture flux into NEB are reduced. But the intensified meridional moisture flux contributes to increase the NEB moisture amount. This, associated with an increased upward motion, contributes toward sustaining a more intensive convective activity.

The different correlation patterns obtained in this study highlight the fact that the relation between heat flux and convective activity is complex, nonlinear, and is not of the same type as in the whole Atlantic basin. The positive correlation is spread over a large region of the northern tropical Atlantic, while the negative correlation remains confined to a limited area of NEB. We explained these patterns with a modification of the atmospheric circulation, particularly trade wind anomalies. The negative correlation should then spread in a larger region, where the southern trade wind anomalies are strong. There seems to be another mechanism, yet to be investigated, that reduces the correlation in the southeastern tropical Atlantic.

The lag correlation study offers interesting results. Although the 1-month lag and the in-phase correlation patterns (Fig. 2) are consistent, there is a significant difference between spatial responses. Indeed, the maximum response moves northward from 5° (1-month lag correlation pattern) to 15°N (in-phase pattern). Further investigation is required to explain such differences. For this purpose, a likely candidate would be the oceanic and atmospheric surface data provided by the PIRATA buoys located in areas of significant correlation. Moreover, a great advantage of PIRATA data is their availability in real time, which is very useful for forecast applications. This study showed the pertinence

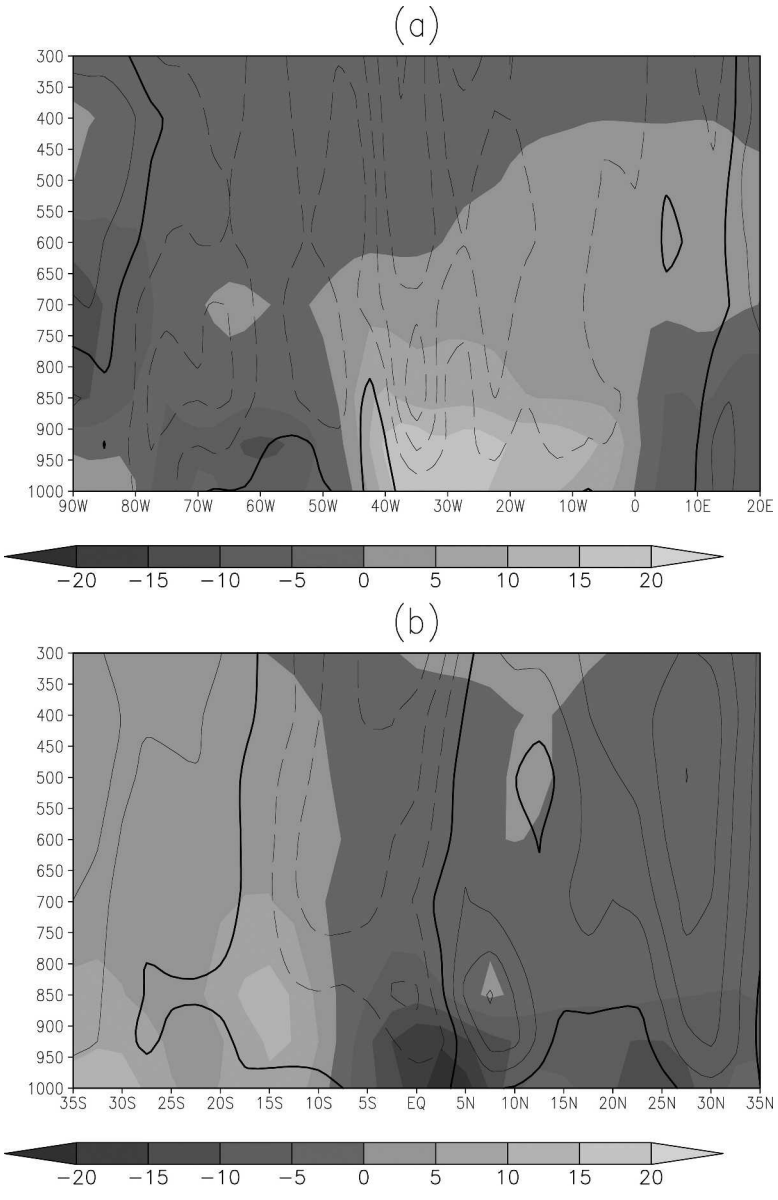

FIG. 4. Bias between flood and drought years of the (a) FMAM zonal moisture flux (10^{-3} g kg^{-1} m s^{-1}; shaded) averaged between 10°S and 0°, and of the (b) FMAM meridional moisture flux (10^{-3} g kg^{-1} m s^{-1}; shaded) averaged between 45° and 35°W. In both cases the black contours represent the bias of the vertical velocity omega (10^{-2} Pa s^{-1}). Contour interval is 0.5 Pa s^{-1}, negative contours (upward bias) are dashed, and the 0 Pa s^{-1} contour is highlighted.

of the four buoys located between 4° and 15°N at 38°W: the buoys at 15° and 12°N are in the area of positive in-phase correlation, and the other two at 8° and 4°N are in the area of the positive 1-month lag correlation.

It would be interesting to calculate 1- or 2-week lag correlations. This temporal scale is more appropriate for the horizontal transport of humidity from the tropical Atlantic to NEB.

5. Conclusions

The in-phase correlation study between the normalized monthly anomalies of the tropical Atlantic latent heat flux and the convective coverage over NEB during its rainy season (FMAM) shows a dipole signature straddling the ITCZ, quite different from the SST dipole (Servain 1991). The positive pole spreads over a

large area of the northen tropical Atlantic, and the negative pole is confined to a limited area off NEB. This pattern is directly associated with anomalies in atmospheric circulation (particularly the ITCZ position and the intensity of the trade winds) that, in turn, drive anomalies of the latent heat flux and NEB convection. Further study will aim at understanding the difference in the spatial expansion of the positive and the negative poles.

A dipole structure is also found in the case of the 1-month lag correlation (the latent heat flux in advance in relation to the convective coverage). However, there are interesting differences in the localization and the spatial expansion of the northern positive pole. The 1-month lag pattern spreads over a narrow area along 5°N between 50° and 10°W, while the in-phase pattern spreads over a more extensive region from the northern coast of South America and west of 32°W. This shows that the response does not result only from a persistent phenomenon and that forecast application should be further investigated.

The analysis of the horizontal moisture flux shows that the additional humidity in the NEB region during flood years does not come from a westward inflow, but from additional southward and northward contributions. Flood years are also characterized by an increased ascending movement over NEB, which helps convective activity.

This study shows the pertinence of the position of the PIRATA moorings along 38°W, located in the region of the maximum in-phase and 1-month lag positive correlations. The PIRATA observations allow calculation of the latent heat and surface moisture fluxes. But the series available at the moment are not long enough to calculate climatologies and normalized anomalies. Longer time series could certainly help performance of forecasting experiments.

Acknowledgments. This work was done in a cooperative framework between the Conselho Nacional de Desenvolvimento Científico e Tecnológico (CNPq), Brazil, and the Institut de Recherche pour le Développement (IRD), France. This study was also supported by the Fundação Cearense de Meteorologia e Recursos Hídricos (FUNCEME) Fortaleza, Brazil, and Fundação Cearense de Apoio ao Desenvolvimento Científico e Tecnológico (FUNCAP), Fortaleza, Brazil, Project Number 002/2003. Thanks to the three anonymous reviewers who helped to improve this manuscript.

REFERENCES

Chung, J. C., 1982: Correlation between the Tropical Atlantic trade winds and precipitation in Northeastern Brazil. *J. Climatol.,* **2,** 35–46.

da Silva, A. M., C. C. Young, and S. Levitus, 1994: *Algorithms and Procedures*. Vol. 1, *Atlas of Surface Marine Data*, NOAA Atlas NESDIS 1, 74 pp.

Durand, B., H. Laurent, L. A. T. Machado, and J. Servain, 2002: Relações entre os fluxos de calor na superfície do Atlântico Tropical e a cobertura de nuvens. *Proc. Anais do XII Congresso Brasileiro de Meteorologia*, Foz do Iguaçu, Brazil, Sociedade Brasileira de Meteorologia, CD-ROM.

Harzallah, A., J. O. R. Aragão, and R. Sadourny, 1996: Interannual rainfall variability in Northeast Brazil: Observation and model simulation. *Int. J. Climatol.,* **16,** 861–878.

Hastenrath, S., and L. Heller, 1977: Dynamics of climatic hazards in Northeast Brazil. *Quart. J. Roy. Meteor. Soc.,* **103,** 77–92.

Kalnay, E., and Coauthors, 1996: The NCEP/NCAR 40-Year Reanalysis Project. *Bull. Amer. Meteor. Soc.,* **77,** 437–471.

Kousky, V. E., 1979: Frontal influences on northeast Brazil. *Mon. Wea. Rev.,* **107,** 1140–1153.

Machado, L. A. T., H. Laurent, N. Dessay, and I. Miranda, 2004: Seasonal and diurnal variability of convection over the Amazonia: A comparison of different vegetation types and large scale forcing. *Theor. Appl. Climatol.,* **78,** doi:10.1007/s00704-004-0044-9.

Moura, A. D., and J. Shukla, 1981: On the dynamics of droughts in northeast Brazil: Observations, theory and numerical experiments with a general circulation model. *J. Atmos. Sci.,* **38,** 2653–2675.

Rotunno, R., and K. A. Emanuel, 1987: An air–sea interaction theory for tropical cyclones. *J. Atmos. Sci.,* **44,** 542–561.

Roucou, P., J. O. R. Aragão, A. Harzallah, B. Fontaine, and S. Janicot, 1996: Vertical motion changes related to Northeast Brazil rainfall variability: A GCM simulation. *Int. J. Climatol.,* **16,** 879–891.

Schiffer, R. A., and W. B. Rossow, 1985: ISCCP global radiance data set: A new resource for climate research. *Bull. Amer. Meteor. Soc.,* **66,** 1498–1505.

Servain, J., 1991: Simple climatic indices for the tropical Atlantic Ocean and some applications. *J. Geophys. Res.,* **96,** 15 137–15 146.

——, A. J. Busalacchi, M. J. McPhaden, A. D. Moura, G. Reverdin, M. Vianna, and S. E. Zebiak, 1998: A Pilot Moored Array in the Tropical Atlantic (PIRATA). *Bull. Amer. Meteor. Soc.,* **79,** 2019–2031.

——, I. Wainer, L. H. Ayina, and H. Roquet, 2000: Relationship between the simulated climatic variability modes of the Tropical Atlantic. *Int. J. Climatol.,* **20,** 939–953.

Strang, D. M. G., 1972: Climatological analysis of rainfall normals in northeastern Brazil. Tech. Rep. IAE-M-O1/72, 70 pp. [Available from Centro Técnico Aeroespacial, 12200 São José dos Campos, SP, Brazil.]

Tao, W.-K., J. Simpson, and S.-T. Soong, 1991: Numerical simulation of a subtropical squall line over the Taiwan Strait. *Mon. Wea. Rev.,* **119,** 2699–2723.

Wang, Y., W.-K. Tao, and J. Simpson, 1996: The impact of ocean surface fluxes on a TOGA COARE convective system. *Mon. Wea. Rev.,* **124,** 2753–2763.

Webster, P. J., and R. Lukas, 1992: TOGA COARE: The Coupled Ocean–Atmosphere Response Experiment. *Bull. Amer. Meteor. Soc.,* **73,** 1377–1416.